

Seasonal variations in the north toroidal sporadic meteor source

M. CAMPBELL-BROWN* and P. WIEGERT

Department of Physics and Astronomy, University of Western Ontario, London, ON, Canada

*Corresponding author. E-mail: margaret.campbell@uwo.ca

(Received 09 March 2009; revision accepted 24 May 2009)

Abstract—Determining the origins of the sporadic meteoroid sources helps determine their current properties. We have analyzed four years of orbital radar data, looking at how the rates, radiants, and orbits of meteoroids in the north toroidal sporadic source change throughout the year. Twelve broad radiant concentrations, separated in either time or radiant location, are identified. Six are broad distributions associated with more focused shower activity, and six are not associated with major showers. Four of the six concentrations not associated with showers have been named Toroidal, Toroidal A, Toroidal B, and Toroidal C, because of their constant location at the north toroidal centre. The other two, which appear close to the north toroidal source and drift toward the helion and antihelion sources respectively, have been named the Helion Arc and the Antihelion Arc. The twelve radiant concentrations generally last for more than ten degrees solar longitude, and those which may have a single parent are likely composed of orbitally evolved material.

INTRODUCTION

Sporadic meteoroids are usually defined as those meteoroids which do not belong to any recognized meteoroid stream. They dominate the flux of meteoroids at the Earth. The distribution of sporadic radiants in the sky is not random; most sporadic meteors have radiants in one of six radiant concentrations, often called the sporadic sources. Each of these sources is produced by the diffusion of meteoroids out of collimated meteoroid streams. The activity of each source varies through the year (Campbell-Brown and Jones 2006). The boundary between shower and sporadic meteors is necessarily arbitrary: generally some threshold for association in radiant and speed is chosen, but there is no agreed-upon standard. It is particularly interesting to try to link sporadic meteoroids, if not with a particular parent, at least with a particular class of parent body. The advanced evolutionary state of most sporadic meteoroid orbits probably precludes determining the specific parent body, but in some cases it may be possible. Finding the parents of the sporadic meteoroid complex allows modeling of its evolution, and makes predictions of the sporadic meteoroid flux away from 1 AU possible.

The apex sources are produced by retrograde meteoroid streams, mainly from Halley-family comets. The helion and antihelion sources are mainly composed of particles from Jupiter-family comets, particularly comet 2P/Encke (Jones et al. 2001; Wiegert et al. 2009). Jones et al. (2001)

concluded that the toroidal sources can be explained as the interaction between a decreasing number of short period comets at high inclinations and the increased probability of observing higher inclination meteoroids due to their higher encounter velocities with the Earth; no specific comets were proposed as sources. The toroidal sources can also be modeled using high inclination near-Earth asteroids (Wiegert et al. 2009) and Jupiter-family comets (Wiegert 2008), but the immediate parent bodies of the toroidal sources are less well determined than those of the other sources. It is possible that the principal parent body or bodies of these sources no longer exist, at least not in the orbit from which material was contributed to the source. The uncertainty in the origin of the toroidal sources leads us to investigate them more thoroughly.

The north toroidal source was first discovered (as a group of high inclination, low eccentricity orbits in meteor radar data from the northern hemisphere) in the early 1960s (Hawkins 1962). The south toroidal source was confirmed in a study of meteor orbit surveys by Jones and Brown (1993), who found it in data from the Adelaide meteor radar; they also characterized the orbital distribution of the north toroidal source, for which more data existed. Campbell-Brown (2008) determined from a study of the Canadian Meteor Orbit Radar (CMOR) data that 18% of observed sporadic meteors were north toroidal; the fraction dropped to 10% when corrected for observing biases, since high latitude radiants are better observed from the northern hemisphere than radiants on the

ecliptic. Brown and Jones (1995) determined from Springhill and Christchurch radar data that approximately 6% of sporadic meteors originated in the north toroidal source, and 6% in the south toroidal source, a slightly lower fraction than the most recent results. At smaller masses observed by radial scatter (High Power Large Aperture, or HPLA) radars, both the Jicamarca Radio Observatory (Chau et al. 2007) and Arecibo (Fentzke and Janches 2008) find north and south toroidal meteors to comprise approximately 1% of observed meteors each, though much of that may be due to the steep selection bias with speed. Fentzke and Janches found through modeling that the observed distribution can be fit assuming the north toroidal source produces 10% of the meteoroid flux at the top of the atmosphere, which is consistent with the CMOR results.

In addition to having the least well-known origin, the toroidal sources, being at high inclinations, have the best chance of linking meteoroids with parent bodies. Objects in high inclination orbits are less likely to interact directly with the planets, except through secular effects, so their orbits may be preserved for longer than bodies in the ecliptic. Collisional lifetimes are also higher for objects in high inclination orbits. Finally, there are simply fewer high inclination objects than objects orbiting in the ecliptic, making unique associations easier.

The largest data set of sporadic meteor orbits comes from CMOR, with a limiting mass of 10^{-7} kg at 30 km s^{-1} . We have analyzed orbital data taken between May 2002 and February 2008. Only north toroidal orbits are available in significant numbers because of the latitude of the radar site; the south toroidal source is below the horizon.

OBSERVATIONS

The CMOR radar began operating in orbital mode in May of 2002, and collected a total of 2.5 million high-quality orbits up to February 2008, the period covered by this initial study. The orbital system operates at 29.85 MHz and consists of a single transmitter which scatters specularly from meteor trails, an interferometer to obtain the direction of echoes to within 2 degrees, and two remote receivers (6 and 8 km from the main site), the time delays from which can be used to compute the trajectory of the meteoroid (Jones et al. 2005). The remote receivers transmit back to the main station over microwave links. Velocities measured in this way have errors of order 5%, and need to be corrected for deceleration, since the portion of ionized trail which is measured represents the motion of the meteoroid after it has passed through a significant amount of atmosphere. This is done statistically (Brown et al. 2004), based on observations of many showers with known velocities. The orbits obtained with CMOR have larger uncertainties than those obtained photographically, particularly in semimajor axis, which is very sensitive to the measured speed. Nevertheless, the large number of orbits

collected provide very good statistics. In a subset of the orbits (3.4×10^5 , about 14%), Fresnel oscillations could be used to independently measure the speed. Those orbits where the Fresnel and time-of-flight speeds agree to within 5 km s^{-1} are expected to be of the highest quality. Errors in the speeds of those meteors which did not meet this criterion may be as high as 20%.

To look at variations of the activity of the north toroidal source with season, some measure of the collecting area as a function of solar longitude is needed. This is not a trivial task, since the power of the microwave links to the remote receivers depends on the weather conditions. A very simple approach was adopted, counting the number of hours in each bin of 10 degrees solar longitude in which 10 or more orbits were recorded. It was found that this number was nearly constant if the years 2002 and 2003 were excluded from the data set (Fig. 1). There is a slight undersampling around 140 degrees solar longitude, and again around 340 degrees, and a slight oversampling around 280 degrees, but otherwise the rate of data collection is nearly uniform. This analysis is not sufficient to calculate the flux of north toroidal meteoroids, since it does not take into account whether the hours observed were favorable for observing the north toroidal source, but it can be used to verify that peaks and troughs in the rates are not due to much larger or smaller data collection times. The collecting area of the north toroidal source for single station observations has a broad maximum around solar longitude 180 and a broad minimum around solar longitude 0. The maximum is less than a factor of two greater than the minimum. The collecting area for the orbital system is expected to follow similar trends, but has not been computed.

RESULTS

Activity

The total number of orbits within 15 degrees of the centre of the north toroidal source in each bin of 10 degrees solar longitude from 2004 to 2008 is shown in Fig. 2. The toroidal activity is independent of the hours observed, except around solar longitude 350, when the drop in the number of recorded orbits may be due to a reduction in the number of hours observed. Also, the number of toroidal orbits changes little from year to year, implying that there were no major losses of data in any year, and that the activity of the north toroidal source is not highly variable from one year to the next.

The most prominent feature in the plot is the spike between 280 and 290 degrees solar longitude. This is due to the most active shower with a radiant in the north toroidal source, the Quadrantids. Even though the duration of the peak of the shower is much smaller than the bin (less than one degree solar longitude), the flux is so high that it dominates

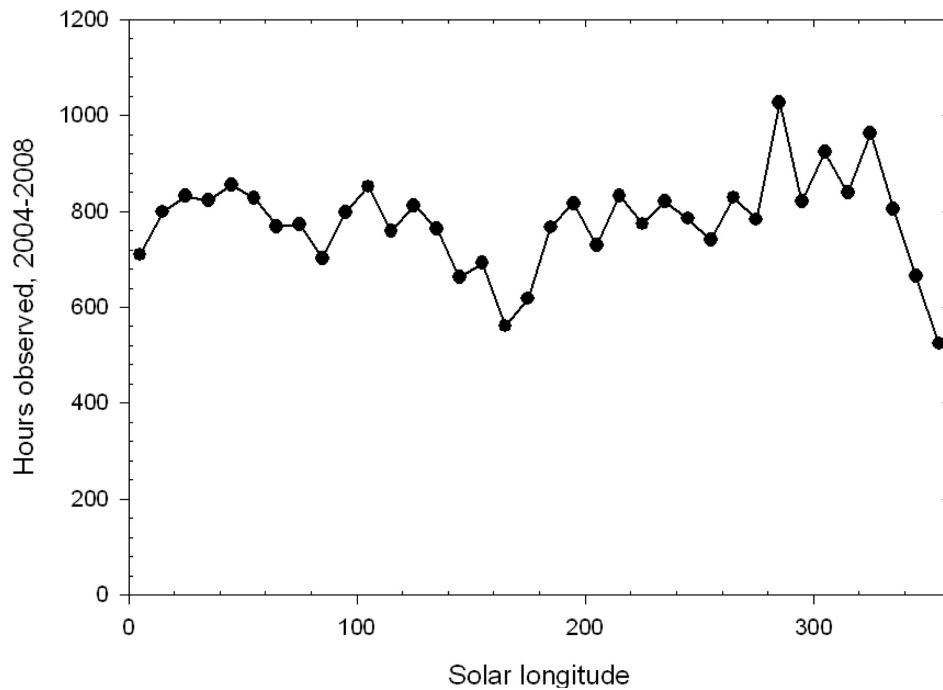


Fig. 1. Total number of hours observed in each bin of 10 degrees solar longitude, using the CMOR orbital system from January 2004 to February 2008.

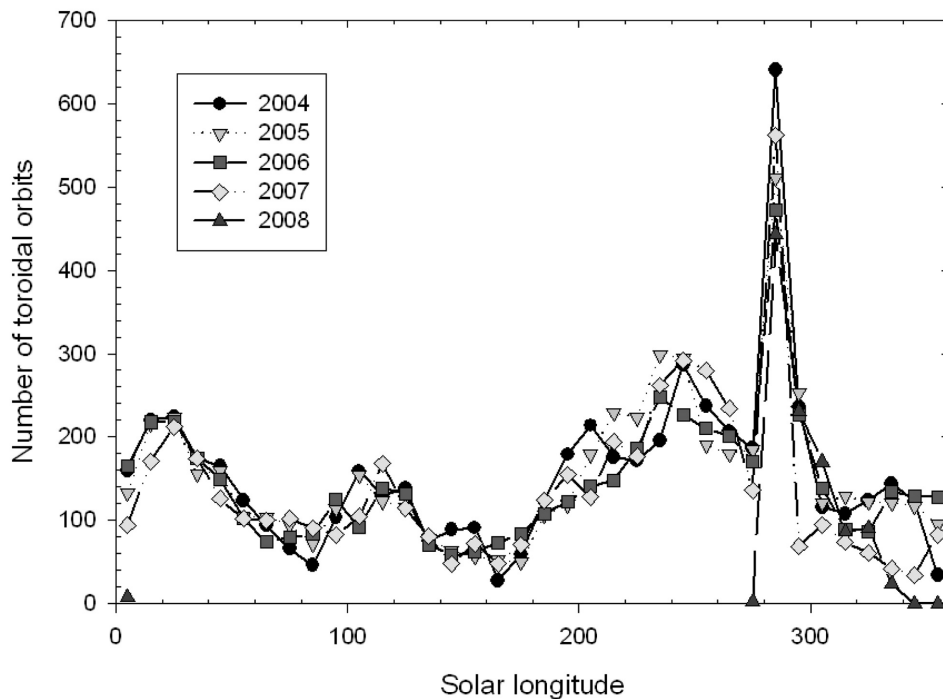


Fig. 2. Total number of north toroidal orbits observed by CMOR between January 2004 and February 2008.

even when averaged over the bin. There are three broader peaks in the activity earlier in the year: between 0 and 70 degrees, between 100 and 130 degrees, and between 190 and 280 degrees. The activity after the Quadrantids is low, but not quite at background. Applying a correction for the

collecting area would make the second peak (between 100 and 130 degrees) weaker, and weaken the beginning of the third broad peak, but it would not eliminate any of the peaks. We have not applied the collecting area to the data since it has not been computed for the orbital system; in any case, we are

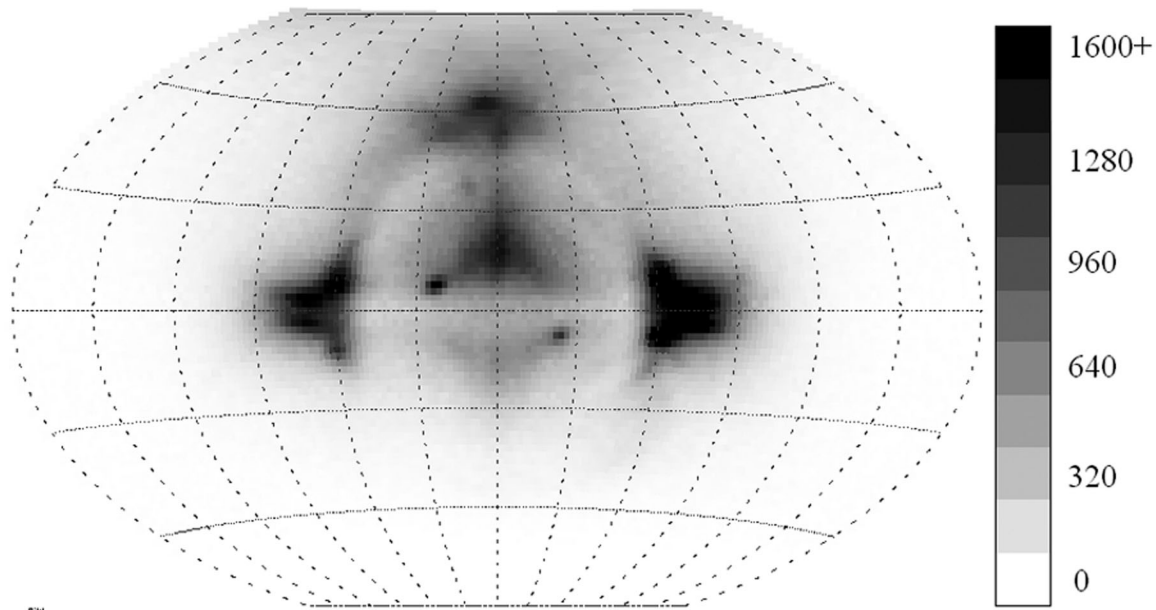


Fig. 3. Radiant density of all CMOR meteor orbits in the study. The equator on the plot is the plane of the ecliptic; the apex of the Earth's way is in the centre and the sun 90 degrees to the left.

not interested, in this study, with the relative strengths of the peaks, but only in their existence.

Radiants and Orbital Elements

The radiants of all the orbits obtained are shown in sun-centered coordinates in Fig. 3. Many showers are visible in the data. The north toroidal source is noticeably offset to the left in the plot, toward the sun. This plot is not corrected for collecting area or observing biases, but these will have little effect on the shape and strength of the north toroidal source.

It is more interesting to look at how the radiant distribution of the north toroidal source changes with season. Figs. 4 and 5 show plots in the same sun-centered ecliptic coordinates, showing the radiants of all orbits in each bin of ten degrees solar longitude. The midpoint of each bin is indicated beside each plot.

The position and number of radiants in the north toroidal source varies with time. The first peak in north toroidal rates (from 0 to 70 degrees solar longitude, which covers the end of March to the end of May) consists of four separate radiant concentrations. The concentration marked A in Fig. 4 we have called the Helion arc, since it moves down in latitude and over in longitude toward the helion source over time. It is strongest between 20 and 30 degrees solar longitude, and moves toward the helion source as it fades. It disappears into the background somewhere around 90 degrees solar longitude. This radiant concentration is not associated with any known shower.

The concentration marked B in Fig. 4 we have called simply Toroidal, since it is centered very nearly on 270, 60,

the average position of the toroidal source. It is weak but visible between 0 and 40 degrees solar longitude.

We initially thought the concentration marked C to be associated with the April Lyrid meteor shower, but close inspection of the 30–40 degrees solar longitude plot shows a small, distinct radiant for the Lyrids just above the larger, more diffuse radiant concentration. We call this the Antihelion arc, since it moves over time down toward the antihelion source. It disappears some time around 80 degrees solar longitude.

The next peak in the rates is due to two radiant concentrations, both of which can be associated with showers. The source marked D is the psi Cassiopeids, and E is the alpha Lacertids.

The next peak is the broadest. In all of these temporal bins, only one radiant concentration is visible; we have split it in two, labeled F and G in Fig. 5. The location of the radiant moves slightly to the north around 220 degrees solar longitude; however, the main reason for the split into two concentrations is the change in orbital elements around this time.

Figure 6 shows the distribution of semimajor axis, eccentricity, inclination and geocentric speed of all orbits with radiants within 15 degrees of the north toroidal source, as a function of solar longitude. The eccentricity is particularly illuminating. The peak in the eccentricity distribution is low (about 0.2) from solar longitude 180 to 200, and moves to higher eccentricity (about 0.8) from 200 to 280. We call the radiant concentration labeled F Toroidal A, since its radiant is very close to the average, and the concentration labeled G Toroidal B. Several showers on the

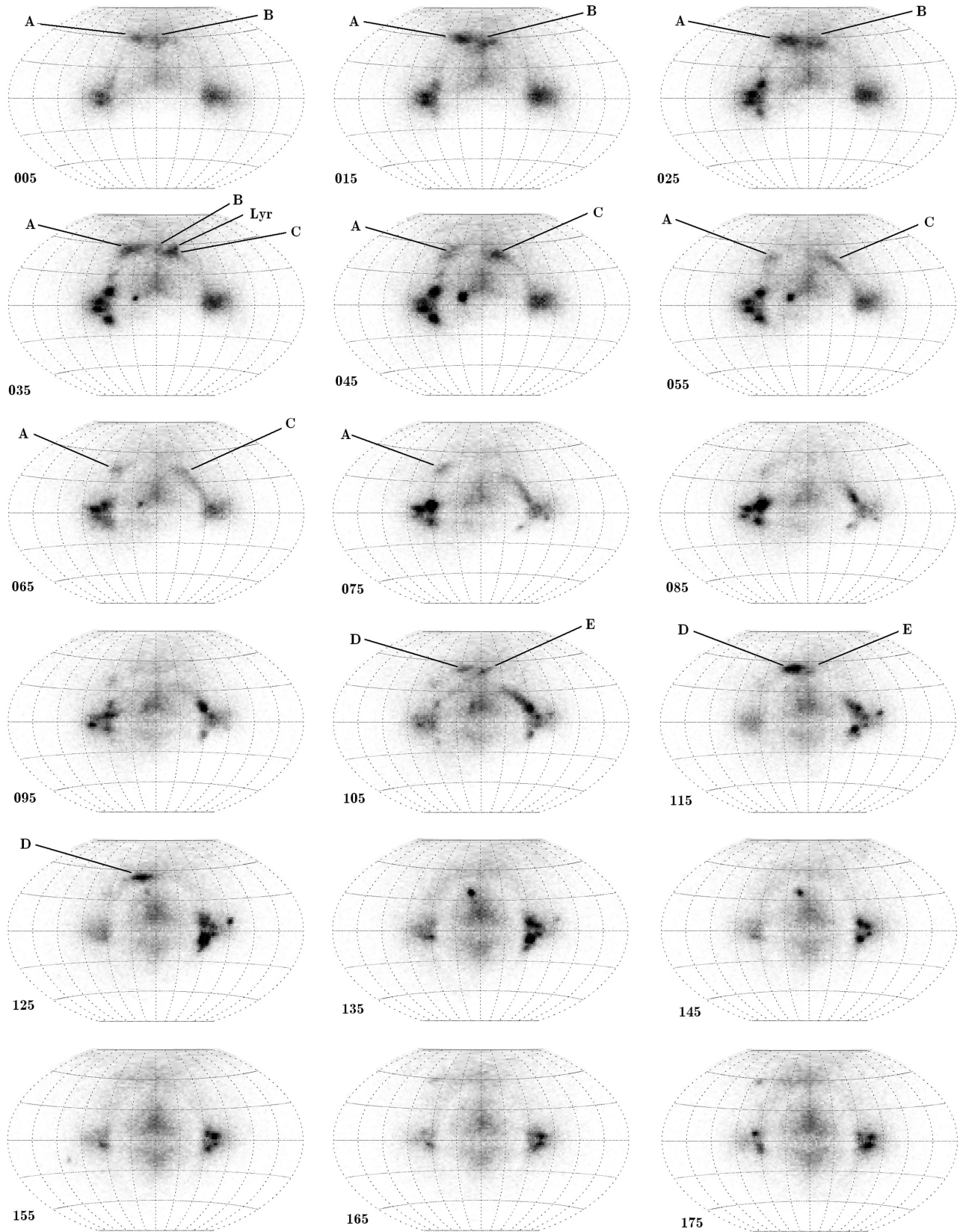


Fig. 4. Radiant plots in bins of ten degrees solar longitude. The solar longitude of the midpoint of each bin is beside each figure. The maximum of the grayscale is 45. A—Helion arc; B—Toroidal; Lyr—April Lyrids; C—Antihelion arc; D—psi Cassiopeids; E—alpha Lacertids.

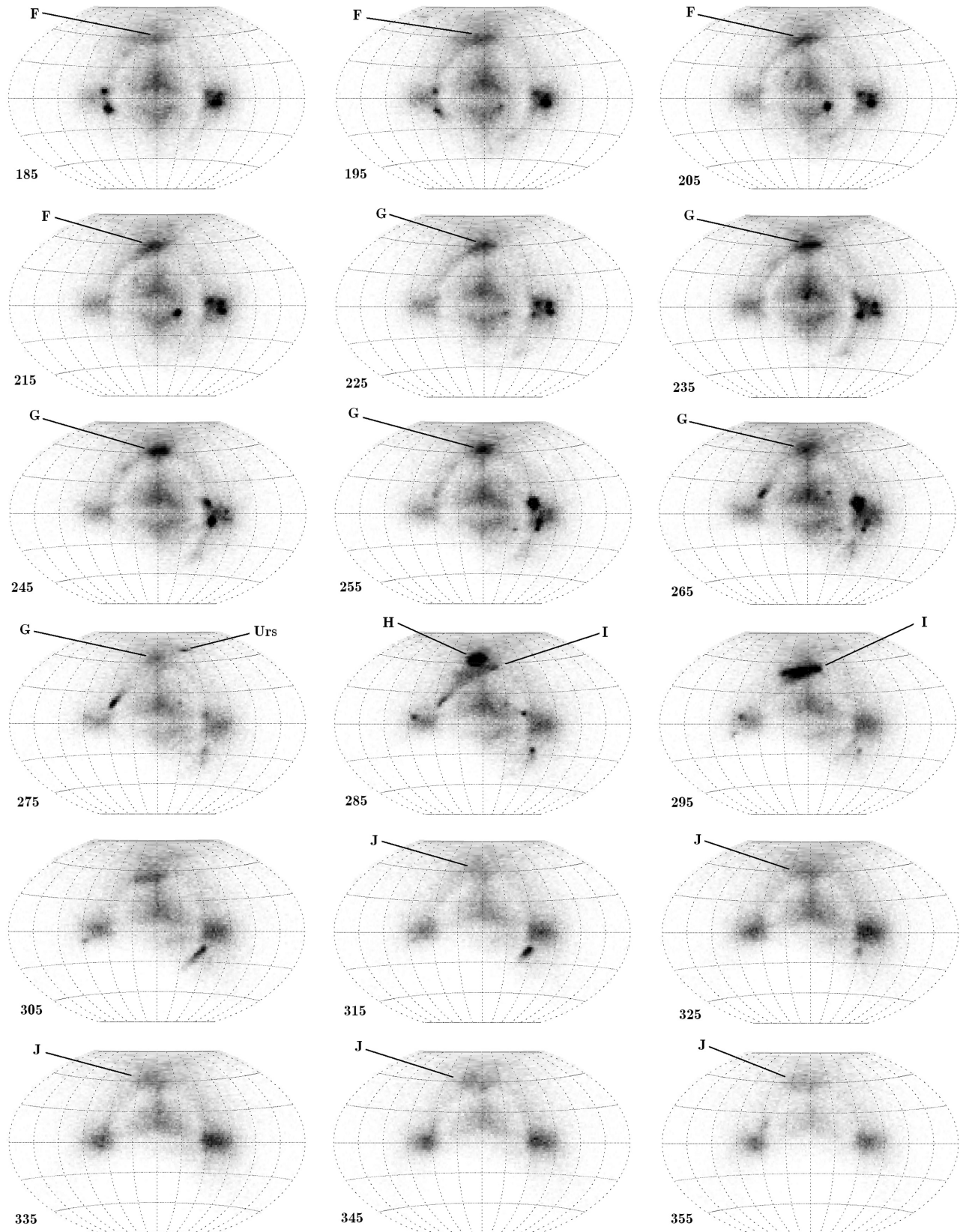


Fig. 5. As in Fig. 4, radiant plots in ten degree solar longitude bins. The maximum of the grayscale is 45. F—Toroidal A; G—Toroidal B; Urs—Ursids; H—Quadrantids; I—theta Corone Borealis, lambda Bootids and xi Corone Borealis; J—Toroidal C.

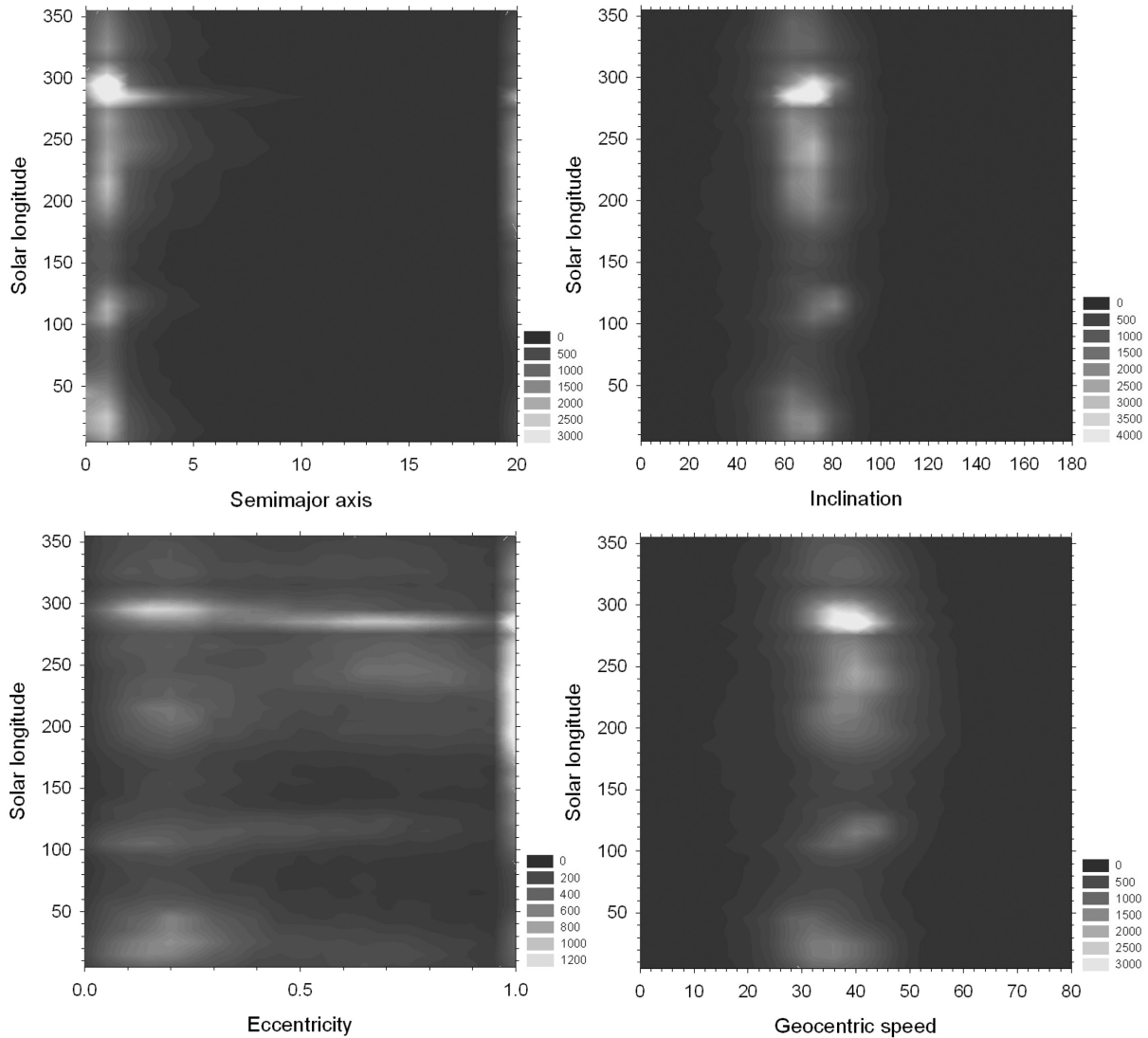


Fig. 6. Orbital element distributions as a function of solar longitude for the north toroidal source. In the semimajor axis and eccentricity plots, the intensity of the final bin in each plot shows the number of orbits with values greater than the maximum (unbound orbits in the case of eccentricity).

IAU list have radiants very close to the Toroidal A concentration: in particular, the October Camelopardalids (ecliptic coordinates 280, 62; peaking at solar longitude 193), an established shower just south of the Toroidal A concentration; and the xi Draconids (at 273, 59, solar longitude 211), a working shower right in the concentration. There are no identified showers with radiants in the Toroidal B concentration: the Ursids become active at the end of the activity period of the Toroidal B concentration, but the radiant is clearly distinct from that radiant concentration. Note that the orbital distributions are not corrected for observing biases. In particular, transverse scatter radars like CMOR are biased against fast meteors which ablate high in the atmosphere, since those trails have a large initial radius and destructive interference from the near and far sides attenuates the echoes, so that fewer are observed. Meteors with radiants in the north

toroidal region, however, have a fairly narrow range of geocentric speeds constrained by observing geometry, so while this effect may slightly shift the peaks in the orbital plots it will not significantly affect the shape of those plots.

The peak in rates which is dominated by the Quadrantids (labeled H in Fig. 5) also includes another radiant concentration, in the form of an extended bar (labeled I). This is composed of three shower radiants (from left to right in the figure): the xi Coronae Borealids, Lambda Bootids, and theta Coronae Borealids. All three showers are part of a single stream complex (Brown et al. 2008).

The last radiant concentration is active from solar longitude 310 to 360, labeled J in Fig. 5. It is called Toroidal C because of its location. Its orbital distribution is distinct from the Toroidal concentration in the first peak, so they do not seem to be a common source artificially separated by a drop in

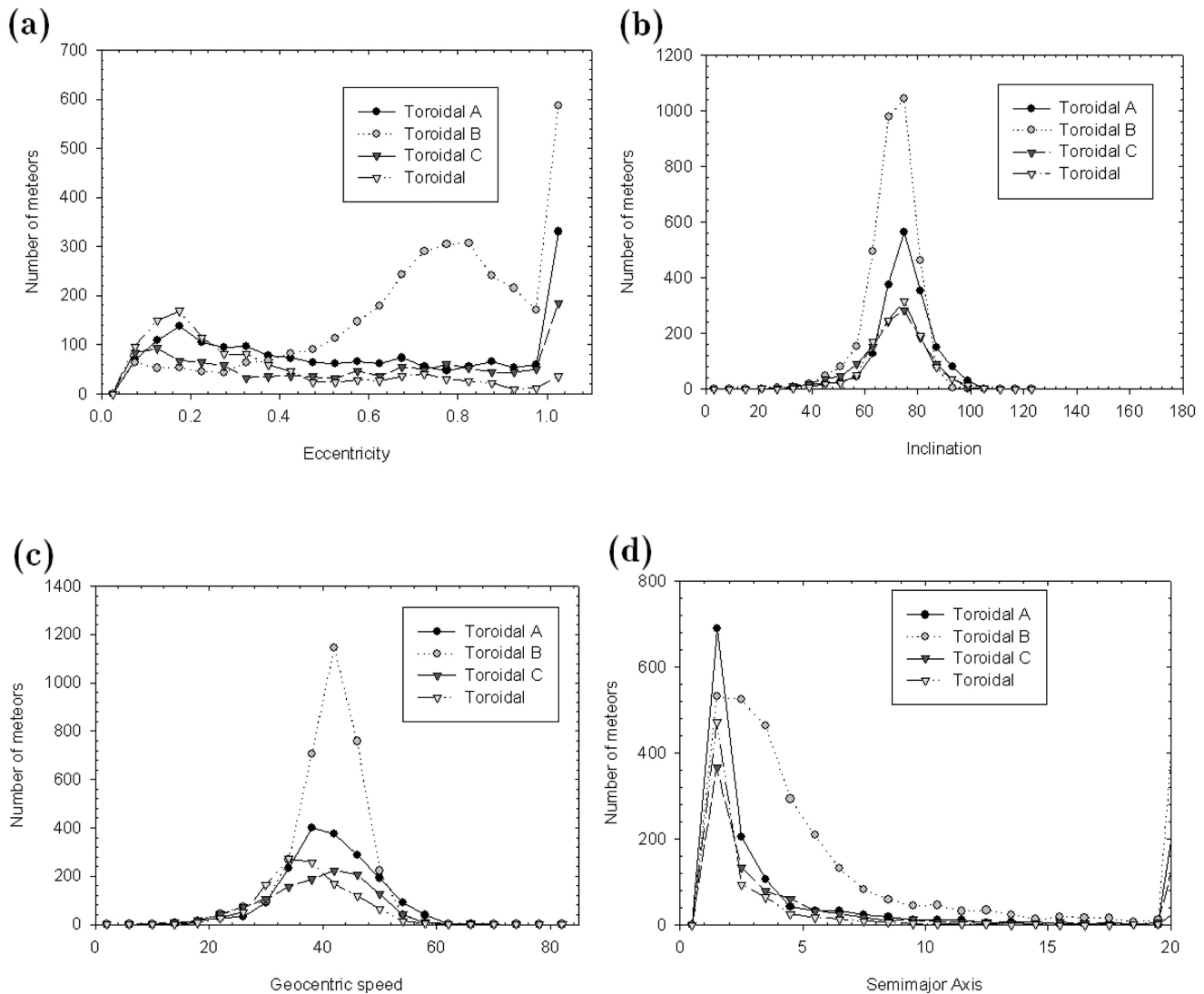


Fig. 7. Distribution of orbital parameters for the four toroidal source radiant concentrations identified as generally Toroidal (see text for the period of activity of each). a) Eccentricity; b) inclination; c) geocentric speed; d) semimajor axis. Note that each of these is a component of the toroidal sporadic source.

rates caused by a lack of observations around 360 degrees solar longitude.

Orbital Distributions of the Radiants

Having identified the radiants which make up the north toroidal source, we can then look more closely at the orbital distribution of each one (particularly when more than one radiant is active). For these we have used the smaller subset of orbits where the Fresnel and time-of-flight speeds agreed to better than 5 km s^{-1} .

In Fig. 7, we compare the orbits of the four Toroidal radiant concentrations. Three of the concentrations (Toroidal, A and C) have similar orbital elements; peaks at low eccentricity (with broad tails), inclinations around 78 degrees, and semimajor axes close to 1 AU. Their geocentric speeds

differ slightly. The Toroidal B concentration has a much higher eccentricity and a larger semimajor axis, and seems to be distinct from the others.

The Helion and Antihelion arc (so called because the radiants drift toward the helion and antihelion points from the north toroidal source) orbital elements are shown in Fig. 8. The helion arc has a broad distribution of eccentricities, and a relatively low inclination (about 70 degrees) and geocentric speed (53 km s^{-1}). The Antihelion arc has eccentricities around 0.3, a high inclination of 80 degrees, and a geocentric speed peaking around 42 km s^{-1} . The semimajor axes of both sources are around 1 AU.

Figure 9 shows the orbital distribution for the concentrations associated with the psi Cassiopeids and alpha Lacertids. The distributions peak close to the measured orbital elements of each shower, which are marked by

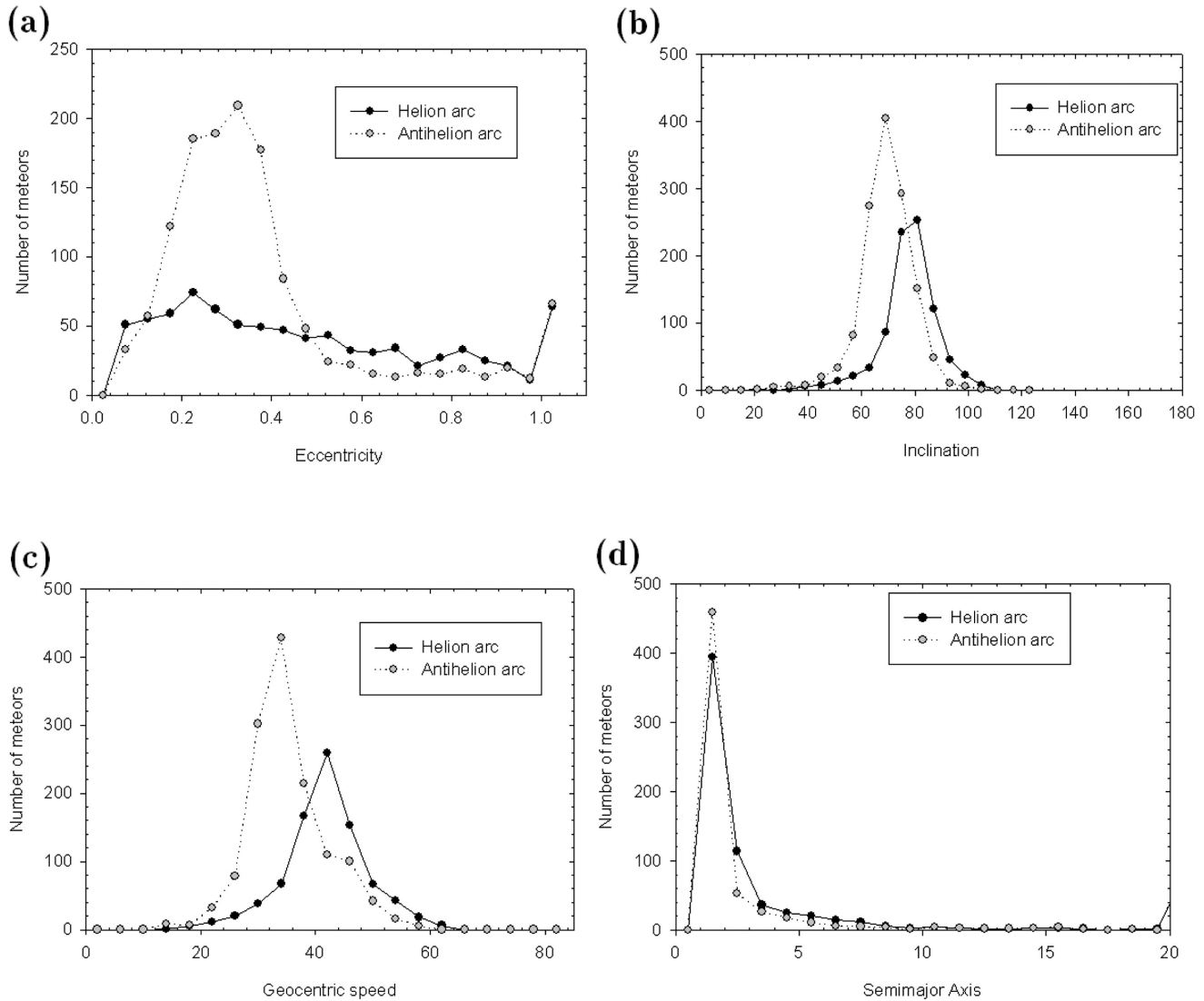


Fig. 8. Orbital element distributions for the Helion arc and antihelion arc.

arrows on the plots. Differences may arise since we are measuring the orbital elements of very broad radiants, and studies of shower meteors tend to accept only meteoroids with a narrow range of radiants and velocities. They may thus be measuring only recent contributions to the stream, while we are also sampling older trails, the orbits of which may have altered over time. CMOR measurements of the psi Cassiopeids (Brown et al. 2008) give $a = 2.2$ AU (slightly higher than the peak in the distribution here, around 1 AU), $e = 0.57$, in the middle of our broad distribution, $i = 83.1^\circ$ (within the uncertainty of our distribution) and $v_g = 44.2$ km s⁻¹, very close to our peak. Similar measurements of the alpha Lacertids have $a = 1.1$ AU (in good agreement), $e = 0.1$ (close to our peak, though we show a long tail to higher eccentricities), $i = 81.8^\circ$ (good agreement) and $v_g = 39.0$ km s⁻¹, slightly lower than our peak.

The orbital distributions of the Quadrantids and

members of the Bootid/Corona Borelid complex are shown in Fig. 10. The theta Corona Borealids were grouped with the lambda Bootids because their radiants are too close together to easily resolve when considering the broad background. The orbital elements for the Quadrantids measured by CMOR ($a = 3.4$ AU, $e = 0.72$, $i = 73^\circ$ and $v_g = 42$ km s⁻¹) fall at the peak of the broader radiant sampled in this study, except for the semimajor axis, which peaks at a slightly lower value for the broader radiant. If we are indeed measuring older meteoroids in the stream, their semimajor axes may be smaller due to Poynting-Robertson drag. The three other showers have very broad eccentricity distributions, which include in each case the measured eccentricity of the shower (shown in Table 1). There is good agreement with the inclinations, where differences among the showers are smaller than the bin size for our histograms. The measured semimajor axes and geocentric speeds of the theta Corona Borealids and lambda

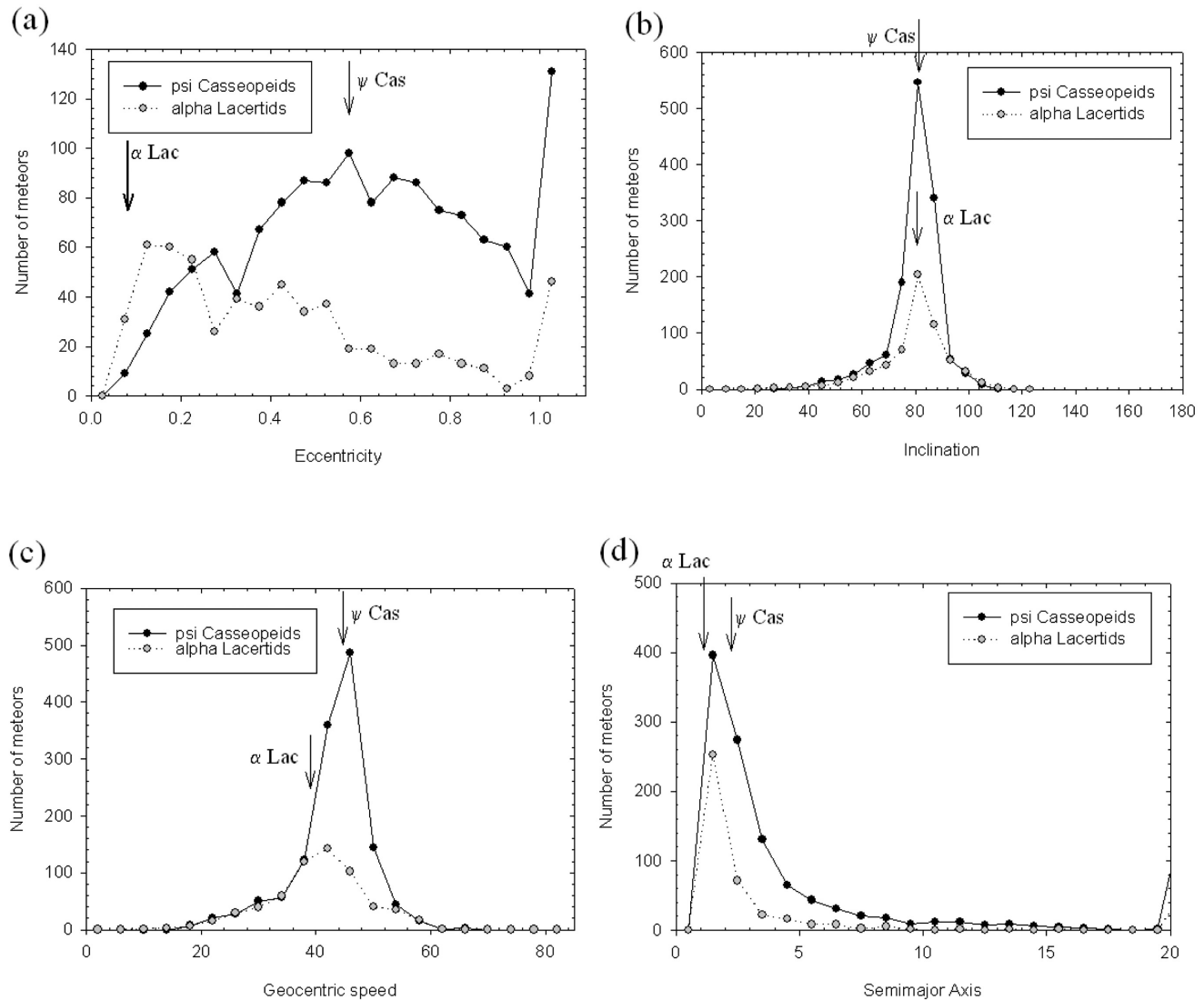


Fig. 9. Orbital elements of the psi Cassiopeids and alpha Lacertids. The positions of the shower orbital elements (from Brown et al. 2008) are shown.

Bootids agree with the peaks in our distributions. For the xi Corona Borealids, both the shower semimajor axis and geocentric speed are slightly higher than the peaks of the broader radiant distribution. The xi Corona Borealids are the broadest of the three radiants, which may account for the difference. Again, we may be sampling a larger range of radiants, while the shower measurements concentrate on a younger, more compact part of the stream.

DISCUSSION

Careful analysis shows that the north toroidal source is composed of distinct radiants and orbital groups which last for relatively brief periods, less than 100 degrees solar longitude. Of the twelve radiant concentrations identified here (not counting the compact April Lyrid and Ursid

radiants), six are composed of the broad background to well-established meteor showers which occur in the north toroidal region; these six have shorter durations (less than 40 degrees solar longitude) than the six sources not associated with established showers. The broad radiants and durations of more than 10 degrees solar longitude for each of those showers likely indicate that they are older showers, with significant spread in orbital parameters due to radiation forces and planetary perturbations. Only the parent of the Quadrantids is currently known, but if the parents of the other showers still exist the connection may be discovered in the future.

Two of the remaining radiant concentrations move along arcs of constant distance to the apex, likely caused by meteoroid streams in Kozai resonances which have their inclination and eccentricity altered by resonances with the

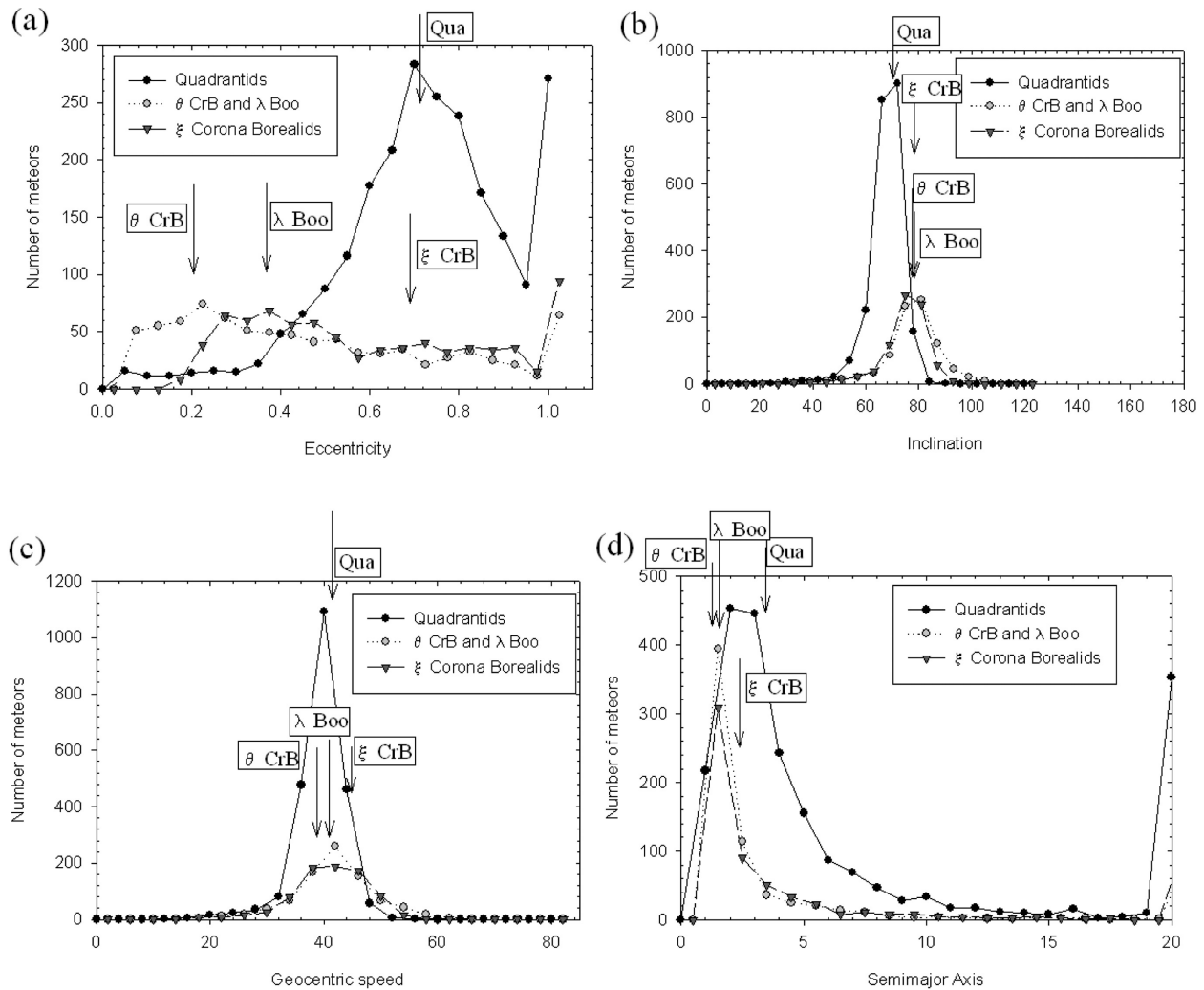


Fig. 10. Orbital distributions for the Quadrantids, combined theta Corona Borealis and lambda Bootids, and the xi Corona Borealis. Elements for the showers are marked with arrows.

planets (Wiegert et al. 2009). Because these sources are of longer duration than any of the shower sources, it is likely that they are even older, and connecting them with parent bodies may be more challenging.

The other four concentrations have fixed radiants close to the centre of the north toroidal source (these are the ones we have labeled Toroidal). While none of these have a major shower associated with them, it's possible that careful analysis of their orbital distribution will determine whether they have single parents or are meteoroids from many parents which are concentrated at the north toroidal point through dynamical processes. The fact that they last less than a fifth of the year may point to fewer parent bodies and more recent separation from those parents.

It may be possible to associate many of the activity concentrations in the north toroidal source with parent bodies. The line between shower and sporadic meteors is somewhat artificial, and many of the sporadic meteors in the north

Table 1. Figure labels for 12 radiant concentrations in the north toroidal sporadic source.

| Label in Figs. 4 and 5 | Name of radiant concentration |
|------------------------|--|
| A | Helion Arc |
| B | Toroidal |
| C | Antihelion Arc |
| D | Psi Cassiopeids |
| E | Alpha Lacertids |
| F | Toroidal A |
| G | Toroidal B |
| H | Quadrantids |
| I | Theta Corone Borealis, lambda Bootids and xi Corone Borealis |
| J | Toroidal C |

toroidal source may be linked to showers in the region. The same analysis may be performed on the apex and helion/antihelion sources, but the larger number of possible parent bodies in the ecliptic plane may make it impossible to

Table 2. Orbital elements of Bootid/Corona Borelid complex showers, as measured with CMOR data (Brown et al. 2008).

| | Semimajor axis a (AU) | Eccentricity e | Inclination i | Geocentric speed v_g (km s ⁻¹) |
|------------------------|----------------------------|------------------|-----------------|---|
| Theta Corona Borealids | 1.1 | 0.21 | 77.1 | 38.6 |
| Lambda Bootids | 1.5 | 0.37 | 79.0 | 41.6 |
| Xi Corona Borealids | 2.6 | 0.67 | 79.4 | 44.5 |

separate out radiant concentrations as we can with the toroidal source. It would be particularly interesting to study the south toroidal source at this level of detail, to determine if it is also composed of specific periods of activity linked to particular radiants and orbital distributions.

Editorial Handling—Dr. Nancy Chabot

REFERENCES

- Brown P. G., Jones J., Weryk R. J., and Campbell-Brown M. D. 2004. The velocity distribution of meteoroids at the Earth as measured by the Canadian Meteor Orbit Radar (CMOR). *Earth, Moon and Planets* 95:639–645.
- Brown P. G., Weryk R. J., Wong D. K., and Jones J. The Canadian Meteor Orbit Radar Meteor Stream Catalogue. *Earth, Moon and Planets* 102:209–219.
- Campbell-Brown M. D. 2008. High resolution radiant distribution and orbits of sporadic radar meteoroids. *Icarus* 196:144–163.
- Campbell-Brown M. D. and Jones J. 2006. Annual variation of sporadic radar meteor rates. *Monthly Notices of the Royal Astronomical Society* 367:709–716.
- Chau J. L., Woodman R. F., and Galindo F. 2006. Sporadic meteor sources as observed by the Jicamarca high-power large-aperture VHF radar. *Icarus* 188:162–174.
- Fentzke J. T. and Janches D. 2008. A semi-empirical model of the contribution from sporadic meteoroid sources on the meteor input function in the MLT observed at Arecibo. *Journal of Geophysical Research* 113:A03304.
- Gartrell G. and Elford W. G. 1975. Southern hemisphere meteor stream determinations. *Australian Journal of Physics* 28:591–620.
- Hawkins G. S. 1962. Radar determination of meteor orbits. *Astronomical Journal* 67:241–244.
- Jones J. and Brown P. 1993. Sporadic meteor radiant distributions: orbital survey results. *Monthly Notices of the Royal Astronomical Society* 265:524–532.
- Jones J., Campbell M., and Nikolova S. 2001. Modelling of the sporadic meteoroid sources. In *Proceedings of the Meteoroids 2001 Conference*, edited by Warmbein B. pp. 575–580.
- Jones J., Brown P., Ellis K. J., Webster A. R., Campbell-Brown M., Krzeminski Z., and Weryk R. J. 2005. The Canadian Meteor Orbit Radar: System overview and preliminary results. *Planetary and Space Science* 53:413–421.
- Wiegert P. 2008. The dynamics of low-perihelion meteoroid streams. *Earth, Moon and Planets* 102:15–26.
- Wiegert P., Vaubaillon J., and Campbell-Brown M. 2009. A dynamical model of the sporadic meteoroid complex. *Icarus* 201: 295–310.